

1 **Experimental Snowball Earth Viscosity Drives the Evolution of Motile Multicellularity**

2

3 Andrea Halling^{1,2*}, Brysyn Goodson¹, Anna Hirschmann³, Boswell A. Wing², Carl Simpson^{2,4}

4

5 ¹Department of Ecology and Evolutionary Biology, University of Colorado Boulder

6 ²Department of Geological Sciences, University of Colorado Boulder

7 ³Department of Applied Mathematics, University of Colorado Boulder

8 ⁴University of Colorado Museum of Natural History, University of Colorado Boulder

9

10 *Corresponding author: andrea.halling@colorado.edu

11

12 **Keywords:** Snowball Earth, multicellularity, viscosity, eukaryotic flagella, division of labor

13

14

15

16

17 **Abstract**

18 During the 70-million-year span of the Cryogenian Snowball Earth glaciations, low ocean temperatures
19 beneath global sea ice increased water viscosity up to fourfold. In the absence of adaptation, unicellular
20 organisms living in this viscous environment were limited in their ability to move and acquire nutrients.
21 We experimentally test the hypothesis that multicellularity evolved in order to overcome this viscosity-
22 induced metabolic deficit. In the presence of Snowball Earth viscosities, we find that populations of
23 unicellular green algae evolve motile multicellular phenotypes in addition to other phenotypes that
24 optimize different combinations of size and speed. As the Snowball Earth subsided and warm seas
25 returned, the novelty of motile multicellularity permitted these organisms to take physical control over
26 their local environment for the first time. This innovation may underpin the evolution of dominant
27 multicellular lineages on Earth today.

28

29

30

31 **Significance statement**

32 Beginning 720-million years ago, two global glaciations — together known as the Snowball Earth —
33 covered the planet with a thick layer of ice for a total of 70-million years. Several groups of complex
34 multicellular organisms independently radiated at this time, including animals, green algae, and red algae.
35 All of these clades include lineages with large bodies made of thousands of cells, multiple cell types, and
36 spatial organization. At first glance, it seems that life merely survived despite the Snowball Earth
37 glaciations. We find experimental evidence that the Snowball Earth glaciations were instead an
38 evolutionary trigger for the diversification of complex multicellular groups.

39 **Introduction**

40 Simple eukaryotic multicellularity has evolved many times in Earth's history (1-3) and easily evolves in
41 response to numerous experimental selective pressures in the lab (4-8). While this experimental and
42 paleontological work has helped demystify the process, it highlights a paradox in our understanding: if
43 multicellularity is so easy to evolve, why did modern multicellular lineages that have dominated
44 ecosystems for the last 540 million years take so long to diversify after the origin of eukaryotes?
45 Investigating the temporally unique geological selective pressures when dominant multicellular lineages
46 radiated can help to resolve this paradox.

47

48 All sources of information on the origins of obligately multicellular eukaryotes are biased in different
49 ways, but the direction of those biases paints a clear picture (9). Molecular clock dates — which tend to
50 be biased toward older dates (10-13) — indicate that the origins of animals occurred within the Tonian,
51 prior to the Snowball Earth Glaciations (14, 15). Early fossilized animals – which tend to be biased
52 toward more recent dates (11-13) – appear in the Cryogenian interglacial interval (16) as well as the
53 Ediacaran after the Snowball Earth glaciations are over (Fig. 1, 16, 17). The molecular clock dates of
54 multicellular green and red algae are clustered in the Tonian-Cryogenian (18, 19). Although some fossils
55 of unclear modern affinity appear earlier in the rock record, small filamentous multicellular algae become
56 common in the Tonian (3, 20-24). In the Cryogenian interglacial Nantou flora, larger algal fossils appear
57 with a significant increase in surface area to volume ratio (20, 25). Collectively, these sources indicate
58 that the early history and radiation of multicellular clades coincide temporally with the Tonian-
59 Cryogenian Snowball Earth interval (Fig. 1).

60

61 The oxygen requirement of modern multicellular organisms has long lead to the inference that oxygen
62 levels increased along with the rise of animals and other multicellular organisms (2, 26, 27). We now
63 know that the significant rise of atmospheric oxygen levels occurred after the Cambrian explosion (28-33)
64 nearly 200-million years too late for it to be the cause of the origin of multicellularity in animals and

65 algae. In addition to this mismatch in timing, high seawater temperatures in the aftermath of the Snowball
66 Earth glaciations would have physiologically limited access to oxygen (34-36). Therefore, the ability for
67 animals to use any increasing oxygen levels would have been suppressed by thermal stress until the
68 oceans cooled sufficiently (37). Furthermore, it has been shown that high levels of oxygen actually
69 suppress the size of experimentally evolved multicellular organisms (38) complicating any mechanism
70 that directly links oxygen to large size.

71
72 It is also hypothesized that continental weathering caused by the Snowball Earth glaciations (39, 40)
73 resulted in a massive increase in nutrient availability selecting for multicellularity, despite a likely much
74 earlier occurrence of high nutrient levels (41). Cryogenian nutrient influx does well to explain the shift
75 from bacterial primary productivity to productivity dominated by eukaryotes (39, 42), but does not easily
76 explain the origin of multicellularity, even if it helps explain the later Cambrian explosion (43). Biotic
77 drivers, such as predation and grazing, are also a common hypothesis for the selection of multicellular
78 eukaryotes (5-7, 44). Yet eukaryotic predation evolved with heterotrophy during eukaryogenesis (45-47)
79 and predates the origin of multicellularity (47, 48). Moreover, unicellular autotrophs often possess the
80 ability to curtail predator-prey arms races (49).

81
82 Prior to the Cryogenian, life would have likely lived predominately in shallow, warm tropical seas (50).
83 As early as 780 mya (51, 52), seawater temperature drastically decreased as the oceans became uniformly
84 cold (53). For organisms adapted to living in warm seawater, this would have become a homogeneous
85 global selective filter. This temperature decrease would result in a global increase of water viscosity (Fig.
86 1). Life could survive under thick sea ice but to access food, organisms would have had to contend with
87 the high viscosity of the seawater.

88
89 With little observed extinction (54) and no spatial refugia (53), populations of Cryogenian unicellular
90 eukaryotes must have adapted to the cold viscous conditions of Snowball Earth in order to overcome the

91 metabolic deficit imposed on them. There are several hypothesized strategies that unicellular organisms
92 could have used in order to minimize this deficit by optimizing size, motility, and metabolic scaling (55,
93 56). Unicells could have become smaller, lowering their metabolic rates to match availability.
94 Alternatively, unicells could have increased nutrient acquisition by becoming multicellular. Larger sizes
95 together with higher collectively generated speeds would have increased encounter rates enough to satisfy
96 metabolic needs of larger bodies (55). Evolution driven by the physical changes of seawater during the
97 Snowball Earth has the potential to explain both the timing and the exclusively eukaryotic nature of
98 complex multicellularity (55, 56).

99

100 To test the biological feasibility of this hypothesis, we isolate the physical aspect of viscosity to use as a
101 selective regime in microbial evolution experiments. Our experimental petri dish (macroplate, Fig. S1),
102 inspired by Baym et al 2016 (57), utilizes a stepwise viscosity gradient. This macroplate spatially
103 represents the temporal increase in viscosity as Snowball Earth conditions set in. Our setup provides a
104 stable gradient over the timescale of weeks to months as diffusion of our viscosity-inducing polymer
105 (Ficoll400) occurs slowly, as a function of length squared. We inoculate wildtype *Chlamydomonas*
106 *reinhardtii* — a unicellular green alga — at the standard viscosity (1x) of HSA media in the center of the
107 circular Macroplate. As the population grows out radially, only individuals with the ability to move into
108 the sections of higher viscosity (2x and 4x relative viscosities) continue to propagate. The spatially
109 structured environment of the Macroplate acts as a vehicle for experimental evolution, with viscosity as
110 the selective barrier, and nutrient availability as the evolutionary driver.

111

112 **Results**

113 We observe that *C. reinhardtii* evolves a diversity of phenotypic responses to media of 2x and 4x relative
114 viscosities. This includes flagellated motile colonies of four and eight cells, small non-motile unicells, and
115 macroscopic non-motile colonies. Coulter Counter size distributions as well as microscopy of the
116 populations living within the 2x and 4x sections of the macroplate reflect this phenotypic shift (Fig. 2).

117
118 In addition to unique size distributions, seemingly coordinated motility was observed in four and eight-
119 celled individuals from both 2x and 4x relative viscosities (Fig. 3). As expected, (55, 58), single cells
120 decreased in speed as viscosity increased ($\sim 12 \mu\text{m s}^{-1}$ in 1x, $\sim 4 \mu\text{m s}^{-1}$ in 2x, and $\sim 1.7 \mu\text{m s}^{-1}$ in 4x relative
121 viscosities) while colonies of four and eight cells maintain average speeds near $\sim 15 \mu\text{m s}^{-1}$ in 2x and 4x
122 relative viscosities (Movie S1). These motile phenotypes are maintained even when returned to media of
123 1x viscosity and transferred for at least 70 generations (Fig. 4).

124
125 **Discussion**
126 The results of our experiments clearly match two theoretical expectations. The first [1] is that viscosity
127 has a disproportional effect on motility in single cells compared with multicells due to the increase in
128 collective thrust (58-60). As viscosity increases, we observe single cells decrease in speed while
129 multicells do not (Fig. 3). The second [2] expectation met by our experiment is that as viscosity increases,
130 the speed needed to maintain balance between nutrient acquisition and metabolism is equal to the speed of
131 the ancestral unicell in the original low viscosity (55). Not only do we observe a disproportionate effect of
132 viscosity on single cells and multicells, we observe that multicells maintain a speed in high viscosity
133 which, as predicted (55), corresponds to the speed of single cells in 1x viscosity (Fig. 3).

134
135 The high viscosity of Snowball Earth oceans provided a universal selective barrier that could have been
136 overcome using a variety of strategies. As both increased speed and decreased size are possible
137 adaptations for high viscosity, it is not surprising to see these phenotypes — such as fast-moving ciliates
138 (61) and unusually small alpha cyanobacteria (62) - arise at this same time in Earth history. Other
139 eukaryotic adaptive strategies for motility and nutrient acquisition likely evolved during this time as well
140 (45, 48). Many marine macroalgae rely on the surrounding current to bring nutrients to their blades (63);
141 high seawater viscosity may explain the observed increase in surface area to volume ratio in the
142 Cryogenian (20).

143

144 The idea of “complex multicellularity” tends to be entirely phenotypic — defined by large size, division
145 of labor, and spatial organization (2, 64). Although none of the individual phenotypes we evolved in the
146 lab possess all three aspects of complex multicellularity (2, 64), at least two are present independently.
147 Large size is apparent in colonies visible to the naked eye, and spatial organization is present in motile
148 multicellular forms with externally oriented flagella and coordinated behavior. The third aspect of
149 complexity — division of labor – could potentially be present as well. The pre-existing variation of *C.*
150 *reinhardtii*’s metabolism could be utilized evolutionarily, differentiating metabolically in response to
151 nutrient availability or position within a large three-dimensional colony of cells (64-66). Moreover, the
152 flagellar constraint on mitosis (64, 65, 67, 68) may also provide an opportunity for functional division of
153 labor to evolve.

154

155 By this phenotypic definition, we observe “complexity” arise multiple times through Earth history (for
156 example in *Bangiomorpha*, *Proterocladus*, and *Qingshania*). But there is a macroevolutionary facet of
157 complex multicellularity exemplified by dominant modern clades that possess it—that of evolutionary
158 success. Our experiment couples the phenotypic aspects of multicellularity with a relevant environmental
159 pressure in which multicellularity not only evolves, but also provides an advantage to being complex. So
160 why did modern multicellular lineages take so long to diversify if multicellularity is so easy to evolve?
161 Our framework helps to resolve this paradox. The environment to globally select for complex life maybe
162 just didn’t exist until the Snowball Earth.

163

164 Traits we observe to evolve in response to high viscosity, such as heritable multicellularity and organized
165 flagellar orientation, would have also been advantageous in the warm, post-glacial oceans. As glaciers
166 melted at the end of the Cryogenian period, nutrients were rapidly released into coastal waters (69). The
167 resulting eutrophic environments would have led to a burst in primary productivity (39). In this
168 competitive environment, the novelty of becoming larger and moving faster in order to survive the cold,

169 viscous conditions of Snowball Earth oceans would lead to an ecological innovation in the post-Snowball
170 world. Nascent motile multicellular lineages could take advantage of low marine viscosities to manipulate
171 their surroundings (55), feeding in new and previously inaccessible ways. The ability to control the local
172 environment — as opposed to being subject to it — opened the door for the origin and specialization of
173 the dominant multicellular lineages on Earth today.

174

175 **Materials and Methods**

176 *Model Organism:* Before the experiment began, we grew wild-type *C. reinhardtii* CC-125 from the
177 Chlamydomonas Resource Center in 10ml cultures of liquid HSA medium to an optical density (OD750)
178 of 0.7 (~ 2×10^6 cells/mL). We used a 500 nm light plate shaking at 100 rpms to encourage motility.
179 Culture life cycles were not synchronized as we wanted diversity of morphologies present when
180 inoculated into the experimental plate. Four celled colonies are observable during division, but due to the
181 flagellar constraint on division and the presence of the mother cell wall, outward facing flagella that allow
182 for motility are rare. The typical size of a single cell of this strain is around 10 μm in diameter (volume of
183 about 270 μm^3) and we observed speeds of motile individuals ranging from 10 to 40 $\mu\text{m s}^{-1}$.

184

185 *Evolution Experiment:* We designed a large petri plate (24.5 cm in diameter) with radial step changes of
186 increasing viscosity (3.5 cm ring width). Ficoll400 was added to 1.5% agar HSA medium to create a solid
187 base layer with different viscosities in each ring. The hard agar base layer was covered with 3 mm of
188 HSA as a swim layer. We waited three days for the Ficoll400 to diffusively equilibrate between the hard
189 agar layer below and the swim layer above. The plate maintained stable sections of 1x, 2x, and 4x
190 viscosities relative to water at room temperature (25 °C). We placed the plate on to a 500 nm light plate to
191 equilibrate, and when it was ready, 100 μL of culture was used as the inoculant in the center of the plate.
192 *C. reinhardtii* grew for 30 days, corresponding to ~70 generations (10.5-hour gen time) when the
193 population reached the ring of media with 4x the relative viscosity of HSA media. We used a Multisizer

194 4s Coulter Counter to quantify size distributions and light microscopy along with custom motion tracking
195 MATlab code to view and quantify motility.

196

197 *Phenotypic Plasticity Experiments:* As a comparison, we cultured wild type *C. reinhardtii* that had been
198 directly inoculated into the higher viscosity in order to quantify changes due to phenotypic plasticity.
199 Nine 15 mm petri dishes were set up on a 500 nm light plate. Three plates were used for each of the
200 viscosities (1x, 2x, 4x relative viscosities). Cultures grew for approximately 7 generations before 1 ml
201 samples from each were taken for Coulter Counter and microscopy analysis.

202

203 *Media:* We used HSA media from the Chlamydomonas Resource Center and added Ficoll400 in
204 corresponding amounts (0% for 1x, 5.5% for 2x, 9% for 4x) to the solid agar base layer. A single swim
205 layer of HSA media was poured over top to a depth of 3 mm. For the plasticity experiments, Ficoll400
206 was added directly to HSA with the same weight to volume percentages as listed above. Dynamic
207 viscosities of both the macroplate and individual petri dishes used for plasticity were calculated to be
208 0.95cP for 1x, 2.3cP for 2x, and 4.1cP for 4x relative viscosities.

209

210 *Transfers post Experimental Plate:* A transect from the plate with 1x, 2x, and 4x viscosities were
211 transferred into 15 mm petri plates as well as 10 mL culture tubes with corresponding viscosities.
212 Samples were also taken and placed into plates of 1x viscosity in order to observe the stability of
213 phenotypes over time. The stability of the size distributions acts as a measure of the bulk heritability of all
214 phenotypes. These cultures were transferred for ~70 generations in the 1x viscosity before taking Coulter
215 Counter measurements to compare with the wild type *C. reinhardtii* grown in its native 1x viscosity.

216

217 *Coulter Counter:* A sample was taken from each viscosity and we quantified size distributions with a
218 Beckman Coulter Counter Multisizer 4s. 200 μm (20 mL accuvette) and 1000 μm (100 mL beaker)
219 aperture tubes were used with 50 μl and 100 μl of sample respectively to include the full range of sizes

220 from single cells to large colonies. Only the 200 μm aperture tube was used for heritability measurements
221 in order to be able to focus on motile multicellular individuals. Standard operating methods were set to
222 count and measure the individuals in a set volume of 1 ml of sample and electrolyte solution.

223

224 *Microscopy:* We quantify the speed of motile unicells and multicells in each viscosity by randomly
225 selecting sections on a slide and recording 10 second videos under a light microscope. After cleaning the
226 videos of background noise, we used cell tracking code on Matlab to identify size and speed. We counted
227 the number of cells in multicell phenotypes directly from these motility videos.

228

229 **Acknowledgements**

230 The authors would like to thank Adam Younkin for help fabricating the macroplate, Anton P. Avramov,
231 Jeffrey Cameron, Joe Dragavon, and Jian Wei Tay for help with microscopy, Sarah Hurley, Sarah
232 Leventhal, Jinchung Li, Pat Kocielek, and Rebecca Safran for helpful discussion and feedback. AH would
233 like to thank the NSF GRFP.

234 References

- 235 1. N. J. Butterfield, Modes of pre-Ediacaran multicellularity. *Precambrian Research* **173**, 201-211
236 (2009).

237 2. A. H. Knoll, The multiple origins of complex multicellularity. *Annual Review of Earth and*
238 *Planetary Sciences* **39**, 217-239 (2011).

239 3. L. Miao, Z. Yin, A. H. Knoll, Y. Qu, M. Zhu, 1.63-billion-year-old multicellular eukaryotes from
240 the Chuanlinggou Formation in North China. *Science Advances* **10**, eadk3208 (2024).

241 4. W. C. Ratcliff, R. F. Denison, M. Borrello, M. Travisano, Experimental evolution of
242 multicellularity. *Proceedings of the National Academy of Sciences* **109**, 1595-1600 (2012).

243 5. R. Fisher, T. Bell, S. West, Multicellular group formation in response to predators in the alga
244 *Chlorella vulgaris*. *Journal of evolutionary biology* **29**, 551-559 (2016).

245 6. S. E. Kapsetaki, R. M. Fisher, S. A. West, Predation and the formation of multicellular groups in
246 algae. *Evolutionary Ecology Research* **17**, 651-669 (2016).

247 7. M. D. Herron *et al.*, De novo origins of multicellularity in response to predation. *Scientific reports*
248 **9**, 2328 (2019).

249 8. C. J. Rose, K. Hammerschmidt, P. B. Rainey, Experimental evolution of nascent multicellularity:
250 Recognizing a Darwinian transition in individuality. *BioRxiv* (2020).

251 9. M. J. Hopkins, D. W. Bapst, C. Simpson, R. C. Warnock, The inseparability of sampling and time
252 and its influence on attempts to unify the molecular and fossil records. *Paleobiology* **44**, 561-574
253 (2018).

254 10. C. R. Marshall, The fossil record and estimating divergence times between lineages: Maximum
255 divergence times and the importance of reliable phylogenies. *Journal of Molecular Evolution* **30**,
256 400-408 (1990).

257 11. M. Foote, J. Hunter, C. Janis, J. J. Sepkoski, Jr, Evolutionary and preservational constraints on
258 origins of biologic groups: divergence times of eutherian mammals. *Science* **283**, 1310 (1999).

- 259 12. G. E. Budd, R. P. Mann, Two notorious nodes: a critical examination of MCMCTree relaxed
260 molecular clock estimates of the bilaterian animals and placental mammals. *bioRxiv*, 2022.2007.
261 2001.498494 (2022).
- 262 13. M. Pennell (2023) Genes are often uninformative for dating species' origins. (Nature Publishing
263 Group UK London).
- 264 14. M. dos Reis *et al.*, Uncertainty in the timing of origin of animals and the limits of precision in
265 molecular timescales. *Current Biology* **25**, 2939-2950 (2015).
- 266 15. D. B. Mills, W. R. Francis, D. E. Canfield, Animal origins and the Tonian Earth system. *Emerging
267 Topics in Life Sciences* <https://doi.org/10.1042/ETLS20170160>, ETLS20170160 (2018).
- 268 16. G. Burzynski, T. A. Dececchi, G. M. Narbonne, R. W. Dalrymple, Cryogenian Aspidella from
269 northwestern Canada. *Precambrian Research* **336**, 105507 (2020).
- 270 17. N. A. Heim *et al.*, Hierarchical complexity and the size limits of life. *Proc. R. Soc. B* **284**,
271 20171039 (2017).
- 272 18. E. C. Yang *et al.*, Divergence time estimates and the evolution of major lineages in the
273 florideophyte red algae. *Scientific reports* **6**, 21361 (2016).
- 274 19. A. Del Cortona *et al.*, Neoproterozoic origin and multiple transitions to macroscopic growth in
275 green seaweeds. *Proceedings of the National Academy of Sciences* [10.1073/pnas.1910060117](https://doi.org/10.1073/pnas.1910060117),
276 201910060 (2020).
- 277 20. N. Bykova *et al.*, Seaweeds through time: Morphological and ecological analysis of Proterozoic
278 and early Paleozoic benthic macroalgae. *Precambrian Research* **350**, 105875 (2020).
- 279 21. Q. Tang, K. Pang, X. Yuan, S. Xiao, A one-billion-year-old multicellular chlorophyte. *Nature
280 Ecology & Evolution* **4**, 543-549 (2020).
- 281 22. G. Li *et al.*, Tonian carbonaceous compressions indicate that Horodyskia is one of the oldest
282 multicellular and coenocytic macro-organisms. *Communications Biology* **6**, 399 (2023).

- 283 23. J. Liu *et al.*, Macroscopic fossils from the Chuanlinggou Formation of North China: evidence for an
284 earlier origin of multicellular algae in the late Palaeoproterozoic. *Palaeontology* **66**, e12685
285 (2023).
- 286 24. C. Niu *et al.*, Chuaria and Tawuia fossils from~ 1.0 Ga rocks in North China: Implications for a
287 polyphyletic origin of Chuaria and a potential biological link between these two widespread
288 Proterozoic taxa. *Palaeogeography, Palaeoclimatology, Palaeoecology*, 111966 (2023).
- 289 25. Q. Ye *et al.*, The survival of benthic macroscopic phototrophs on a Neoproterozoic snowball Earth.
290 *Geology* **43**, 507-510 (2015).
- 291 26. J. Nursall, Oxygen as a prerequisite to the origin of the Metazoa. *Nature* **183**, 1170 (1959).
- 292 27. K. M. Towe, Oxygen-collagen priority and the early metazoan fossil record. *Proceedings of the
293 National Academy of Sciences* **65**, 781-788 (1970).
- 294 28. E. A. Sperling *et al.*, Oxygen, ecology, and the Cambrian radiation of animals. *Proceedings of the
295 National Academy of Sciences* **110**, 13446-13451 (2013).
- 296 29. A. H. Knoll, E. A. Sperling, Oxygen and animals in Earth history. *Proceedings of the National
297 Academy of Sciences* **111**, 3907-3908 (2014).
- 298 30. D. B. Mills *et al.*, Oxygen requirements of the earliest animals. *Proceedings of the National
299 Academy of Sciences* **111**, 4168-4172 (2014).
- 300 31. D. B. Mills *et al.*, The last common ancestor of animals lacked the HIF pathway and respired in
301 low-oxygen environments. *eLife* **7**, e31176 (2018).
- 302 32. E. A. Sperling, R. G. Stockey, The Temporal and Environmental Context of Early Animal
303 Evolution: Considering All the Ingredients of an “Explosion”. *Integrative and Comparative
304 Biology* **58**, 605-622 (2018).
- 305 33. D. B. Cole *et al.*, On the co-evolution of surface oxygen levels and animals. *Geobiology* (2020).
- 306 34. T. H. Boag, R. G. Stockey, L. E. Elder, P. M. Hull, E. A. Sperling, Oxygen, temperature and the
307 deep-marine stenothermal cradle of Ediacaran evolution. *Proceedings of the Royal Society B* **285**,
308 20181724 (2018).

- 309 35. R. G. Stockey, A. Pohl, A. Ridgwell, S. Finnegan, E. A. Sperling, Decreasing Phanerozoic
310 extinction intensity as a consequence of Earth surface oxygenation and metazoan ecophysiology.
311 *Proceedings of the National Academy of Sciences* **118**, e2101900118 (2021).
- 312 36. E. A. Sperling *et al.*, Breathless through Time: Oxygen and Animals across Earth's History. *The*
313 *Biological Bulletin* **243**, 000-000 (2022).
- 314 37. C. Simpson, Coming together to understand multicellularity. *Trends in Ecology & Evolution* **38**,
315 385-386 (2023).
- 316 38. G. O. Bozdag, E. Libby, R. Pineau, C. T. Reinhard, W. C. Ratcliff, Oxygen suppression of
317 macroscopic multicellularity. *Nature Communications* **12**, 2838 (2021).
- 318 39. J. J. Brocks *et al.*, The rise of algae in Cryogenian oceans and the emergence of animals. *Nature*
319 **548**, 578 (2017).
- 320 40. C. T. Reinhard *et al.*, Evolution of the global phosphorus cycle. *Nature* **541**, 386-389 (2017).
- 321 41. M. Ingalls, J. Grotzinger, T. Present, B. Rasmussen, W. Fischer, Carbonate-Associated Phosphate
322 (CAP) Indicates Elevated Phosphate Availability in Neoarchean Shallow Marine Environments.
323 *Geophysical Research Letters* **49**, e2022GL098100 (2022).
- 324 42. L. K. Eckford-Soper, K. H. Andersen, T. F. Hansen, D. E. Canfield, A case for an active eukaryotic
325 marine biosphere during the Proterozoic era. *Proceedings of the National Academy of Sciences*
326 **119**, e2122042119 (2022).
- 327 43. K. J. Peterson, M. A. McPeek, D. Evans, Tempo and Mode of Early Animal Evolution: Inferences
328 from Rocks, Hox, and Molecular Clocks. *Paleobiology* **31**, 36-55 (2005).
- 329 44. S. M. Stanley, An ecological theory for the sudden origin of multicellular life in the late
330 Precambrian. *Proceedings of the National Academy of Sciences* **70**, 1486-1489 (1973).
- 331 45. S. Porter, The rise of predators. *Geology* **39**, 607-608 (2011).
- 332 46. P. A. Cohen, L. A. Riedman, It's a protist-eat-protist world: recalcitrance, predation, and evolution
333 in the Tonian-Cryogenian ocean. *Emerging Topics in Life Sciences*, ETLS20170145 (2018).
- 334 47. D. B. Mills, The origin of phagocytosis in Earth history. *Interface Focus* **10**, 20200019 (2020).

- 335 48. K. Dumack *et al.*, It's time to consider the Arcellinida shell as a weapon. *European Journal of*
336 *Protistology*, 126051 (2024).
- 337 49. P. Branco, M. Egas, S. R. Hall, J. Huisman, Why do phytoplankton evolve large size in response to
338 grazing? *The American Naturalist* **195**, E20-E37 (2020).
- 339 50. M. LaBarbera, Precambrian geological history and the origin of the Metazoa. *Nature* **273**, 22-25
340 (1978).
- 341 51. E. J. Trower, The enigma of Neoproterozoic giant ooids—Fingerprints of extreme climate?
342 *Geophysical Research Letters*, e2019GL086146 (2020).
- 343 52. E. J. Trower, J. R. Gutoski, V. T. Wala, T. J. Mackey, C. Simpson, Tonian Low-Latitude Marine
344 Ecosystems Were Cold Before Snowball Earth. *Geophysical Research Letters* **50**,
345 e2022GL101903 (2023).
- 346 53. Y. Ashkenazy *et al.*, Dynamics of a Snowball Earth ocean. *Nature* **495**, 90 (2013).
- 347 54. L. A. Riedman, P. M. Sadler, Global species richness record and biostratigraphic potential of early
348 to middle Neoproterozoic eukaryote fossils. *Precambrian Research* **319**, 6-18 (2018).
- 349 55. C. Simpson, Adaptation to a viscous Snowball Earth Ocean as a path to complex multicellularity.
350 *The American Naturalist* **198**, 590-609 (2021).
- 351 56. W. W. Crockett, J. Shaw, C. Simpson, C. P. Kempes, Physical constraints during Snowball Earth
352 drive the evolution of multicellularity. *bioRxiv*, 2023.2012. 2007.570654 (2023).
- 353 57. M. Baym *et al.*, Spatiotemporal microbial evolution on antibiotic landscapes. *Science* **353**, 1147-
354 1151 (2016).
- 355 58. B. Qin, A. Gopinath, J. Yang, J. P. Gollub, P. E. Arratia, Flagellar kinematics and swimming of
356 algal cells in viscoelastic fluids. *Scientific reports* **5**, 9190 (2015).
- 357 59. R. Podolsky, R. Emlet, Separating the effects of temperature and viscosity on swimming and water
358 movement by sand dollar larvae (*Dendraster excentricus*). *Journal of Experimental Biology* **176**,
359 207-222 (1993).

- 360 60. R. D. Podolsky, Temperature and water viscosity: physiological versus mechanical effects on
361 suspension feeding. *Science* **265**, 100-103 (1994).
- 362 61. N. M. Fernandes, C. G. Schrago, A multigene timescale and diversification dynamics of Ciliophora
363 evolution. *Molecular phylogenetics and evolution* **139**, 106521 (2019).
- 364 62. F. O. Aylward, J. C. Uyeda, C. A. Martinez-Gutierrez, A Timeline of Bacterial and Archaeal
365 Diversification in the Ocean. *bioRxiv* (2022).
- 366 63. M. A. Koehl, Ecological biomechanics of marine macrophytes. *Journal of Experimental Botany* **73**,
367 1104-1121 (2022).
- 368 64. J. T. Bonner, *First Signals: The Evolution of Multicellular Development* (Princeton University
369 Press, Princeton, New Jersey, 2001).
- 370 65. J. T. Bonner, On the origin of differentiation. *Journal of biosciences* **28**, 523-528 (2003).
- 371 66. C. D. Schlichting, Origins of differentiation via phenotypic plasticity. *Evolution & development* **5**,
372 98-105 (2003).
- 373 67. V. Koufopanou, The Evolution of Soma in the Volvocales. *American Naturalist* **143**, 907-931
374 (1994).
- 375 68. R. E. Michod, D. Roze, Cooperation and conflict in the evolution of multicellularity. *Heredity* **86**,
376 1-7 (2001).
- 377 69. P. F. Hoffman *et al.*, Snowball Earth climate dynamics and Cryogenian geology-geobiology.
378 *Science Advances* **3**, e1600983 (2017).
- 379 70. M. Dohrmann, G. Wörheide, Dating early animal evolution using phylogenomic data. *Scientific
380 Reports* **7**, 3599 (2017).
- 381 71. N. J. Butterfield, Bangiomorpha pubescens n. gen., n. sp.: implications for the evolution of sex,
382 multicellularity, and the Mesoproterozoic/Neoproterozoic radiation of eukaryotes. *Paleobiology*
383 **26**, 386-404 (2000).

- 384 72. J. Krissansen-Totton, R. Buick, D. C. Catling, A statistical analysis of the carbon isotope record
385 from the Archean to Phanerozoic and implications for the rise of oxygen. *American Journal of*
386 *Science* **315**, 275-316 (2015).
- 387 73. T. M. Lenton, S. J. Daines, B. J. Mills, COPSE reloaded: An improved model of biogeochemical
388 cycling over Phanerozoic time. *Earth-Science Reviews* **178**, 1-28 (2018).
- 389 74. P. W. Crockford *et al.*, Claypool continued: Extending the isotopic record of sedimentary sulfate.
390 *Chemical Geology* **513**, 200-225 (2019).
- 391 75. D. C. Catling, C. R. Glein, K. J. Zahnle, C. P. McKay, Why O₂ Is Required by Complex Life on
392 Habitable Planets and the Concept of Planetary" Oxygenation Time". *Astrobiology* **5**, 415-438
393 (2005).
- 394 76. G. Bell, The origin and early evolution of germ cells as illustrated by the Volvocales. *The origin*
395 *and evolution of sex* **7**, 221-256 (1985).
- 396 77. V. Koufopanou, The evolution of soma in the Volvocales. *The American Naturalist* **143**, 907-931
397 (1994).
- 398
- 399

400 **Figure 1:** Schematic evolution of the Earth System over the billion years of Proterozoic time. 95%
401 confidence intervals for molecular clock divergence time estimates for multicellular lineages (18, 19, 70).
402 Body volume for fossils are split out by prokaryotes (bacteria and archaea), unicellular eukaryotes, and
403 multicellular eukaryotes (17, 55). The earliest multicellular eukaryotic algae, *Protocladus* (21) and
404 *Bangiomorpha* (71) are called out separately. Proxies and modeling provide estimates for CO₂ ppm (72-
405 74)(60, 61, 63) and O₂ ppm (73-75). Inferred seawater viscosity for shallow equatorial ocean with glacial
406 interval viscosities for seawater with temperatures from -4 to -3 °C and salinities of 35 ppt. Interglacial
407 seawater is shown with 35 ppt seawater and temperatures ranging from 25 - 35 °C (55).

408
409
410 **Figure 2:** Size distributions of plastic and evolved populations. Sizes of >13,000 individuals from each
411 plastic population as well as from each radial section from the macroplate. The left side of each density
412 plot (light gray) shows the non-evolved, phenotypic plastic response of *C. reinhardtii* to different levels
413 of viscosity. The right side of each density plot shows the evolved response of *C. reinhardtii* in each
414 viscosity from the macroplate. Separate size distributions are plotted for three sizes of coulter counter
415 aperture tube: 200µm, 1000µm, and 2000µm. For reference, the range and median volume for colonial
416 volvocales (76, 77) are shown as horizontal reference lines.

417
418 **Figure 3:** Quantification of motility in evolved populations. Microscopy videos analyzed by custom cell
419 tracking code were used to find speeds of evolved individuals. Black data points show the decreasing
420 average speeds of single cells from the macroplate in their corresponding increasing viscosities. Blue
421 shows the average speed of motile multicells in 2x relative viscosity and red shows the average speed of
422 motile multicells in 4x relative viscosity Examples of motile phenotypes from evolved populations in 1x,
423 2x, and 4x relative viscosities. Motile unicellular phenotypes were the dominant morphology in the 1x
424 viscosity section of the macroplate. When viscosity increased to 2x relative viscosity, motile multicells of
425 four emerged. In the 4x relative viscosity section of the macroplate, motile multicells of both four and

426 eight cells were abundant in the population. Motility is shown as a stop-frame animation with about 10
427 frames between each image and all phenotypes are displayed on the same scale.

428

429 **Figure 4:** Size distributions of heritability in evolved populations. Wildtype *C. reinhardtii* in 1x viscosity
430 is compared with evolved populations when returned to 1x media and maintained for over 75 generations.
431 The left side of each density plot (light gray) represents the wild-type size distribution. These distributions
432 reflect the return of plastic populations to typical wild-type distributions when placed back into 1x media.
433 The right side of each density plot shows the size distributions of evolved 2x and 4x relative viscosity
434 populations when returned to 1x relative viscosity media. Gray bars show the size range of multicells
435 containing four and eight cells. Motile multicellular phenotypes continued to be abundant in low
436 viscosity.

437

438 **Figure 5:** Evolved multicellular algae possess a multicellular lifecycle. Top row shows stop action stills
439 of a video capturing the asexual reproduction of a single colony. Bottom row, graphical illustration of the
440 same colony, with colors highlighting the daughter cell lineages derived from the cells within the mother
441 colony. Scale bar equals 10 μ m.

Fig. 1

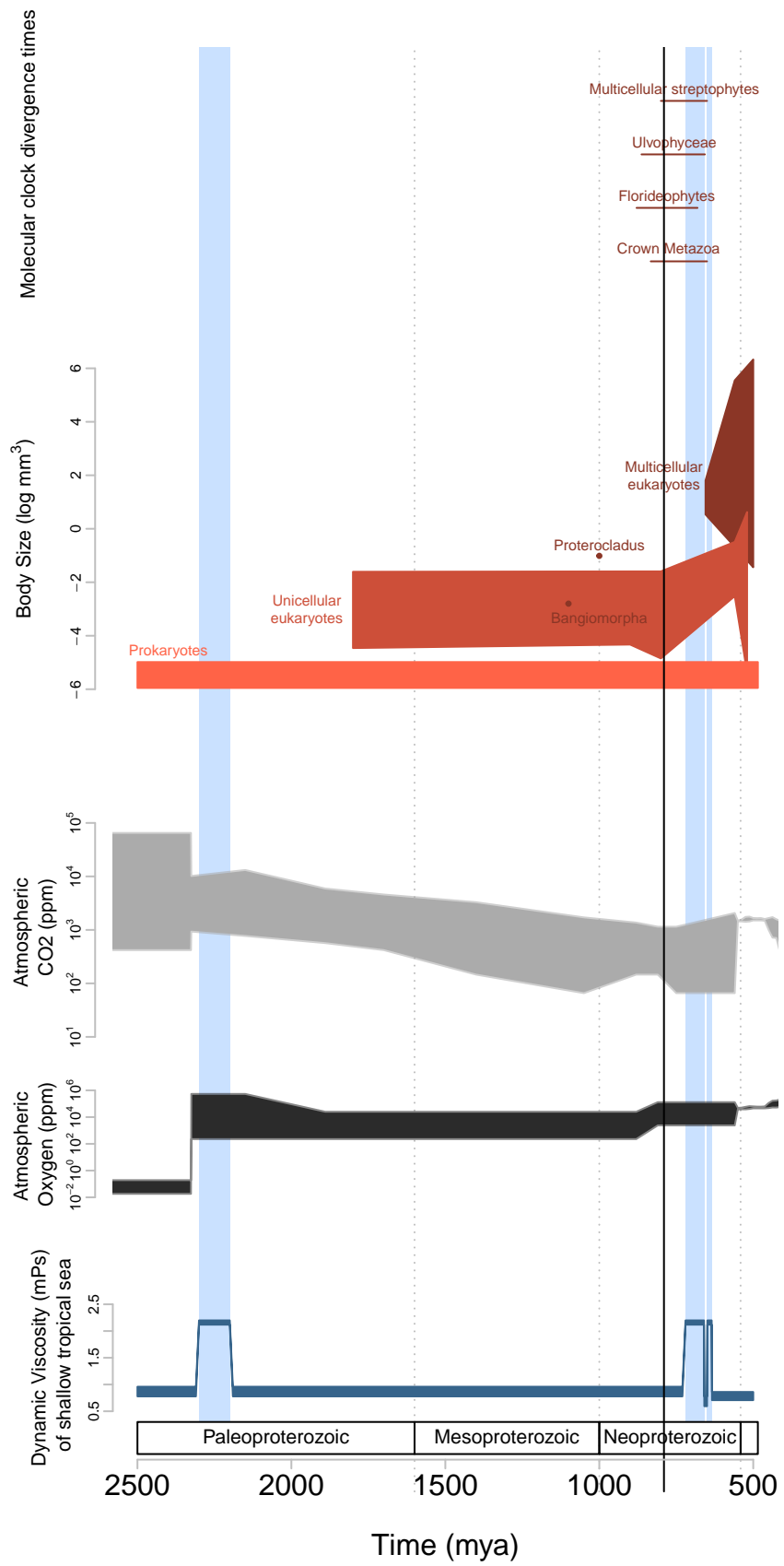


Fig. 2

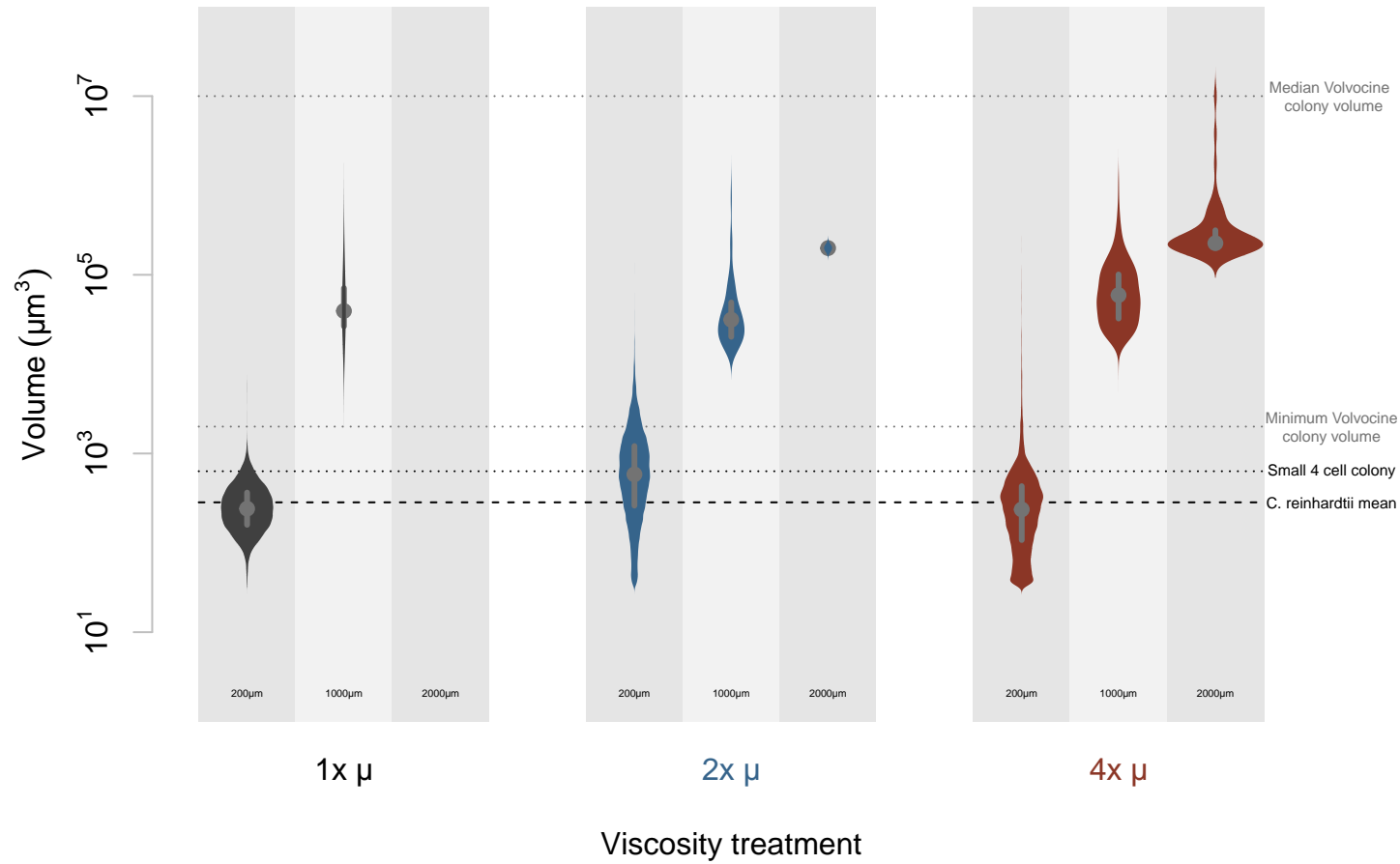


Fig. 3

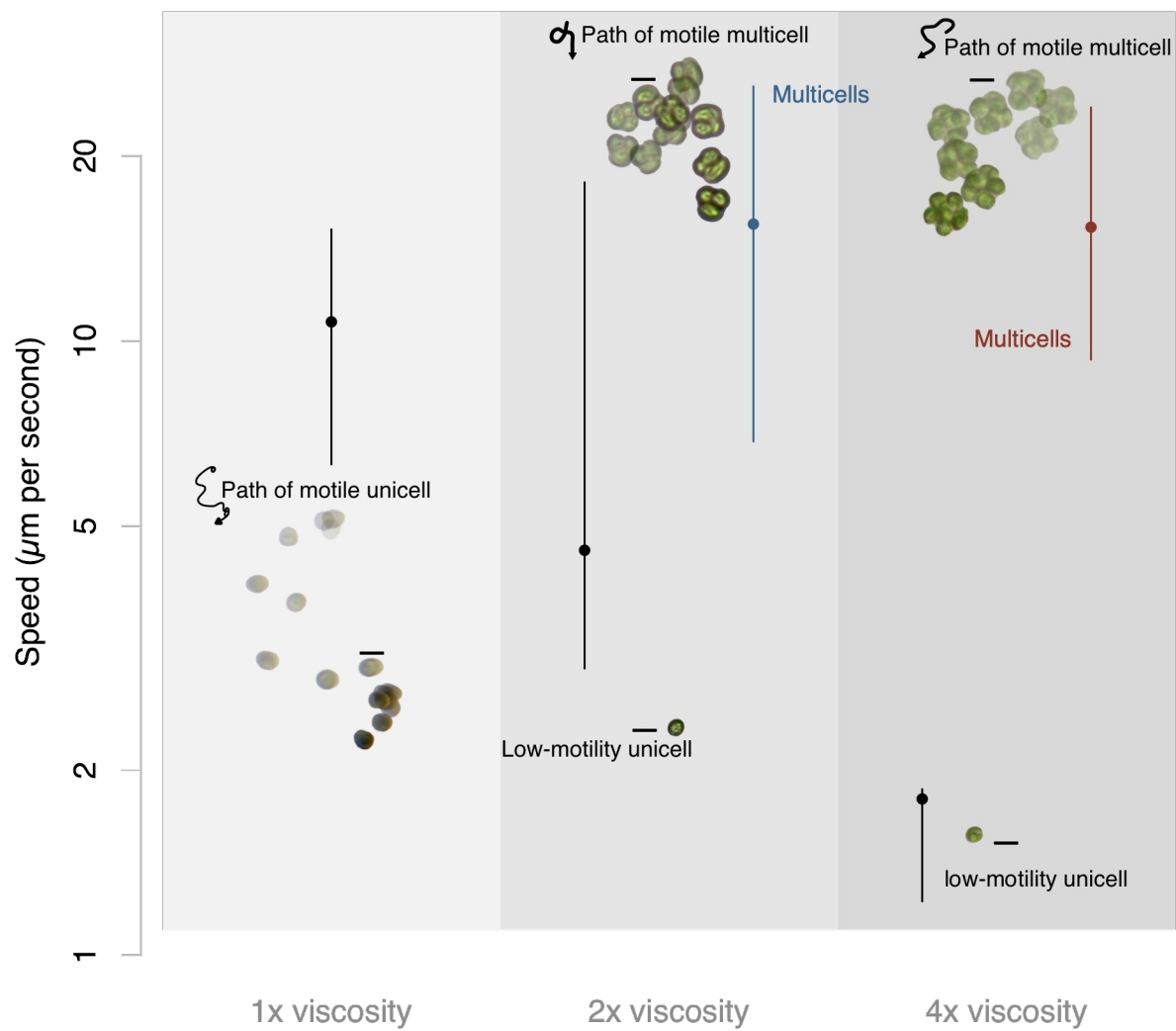


Fig. 4

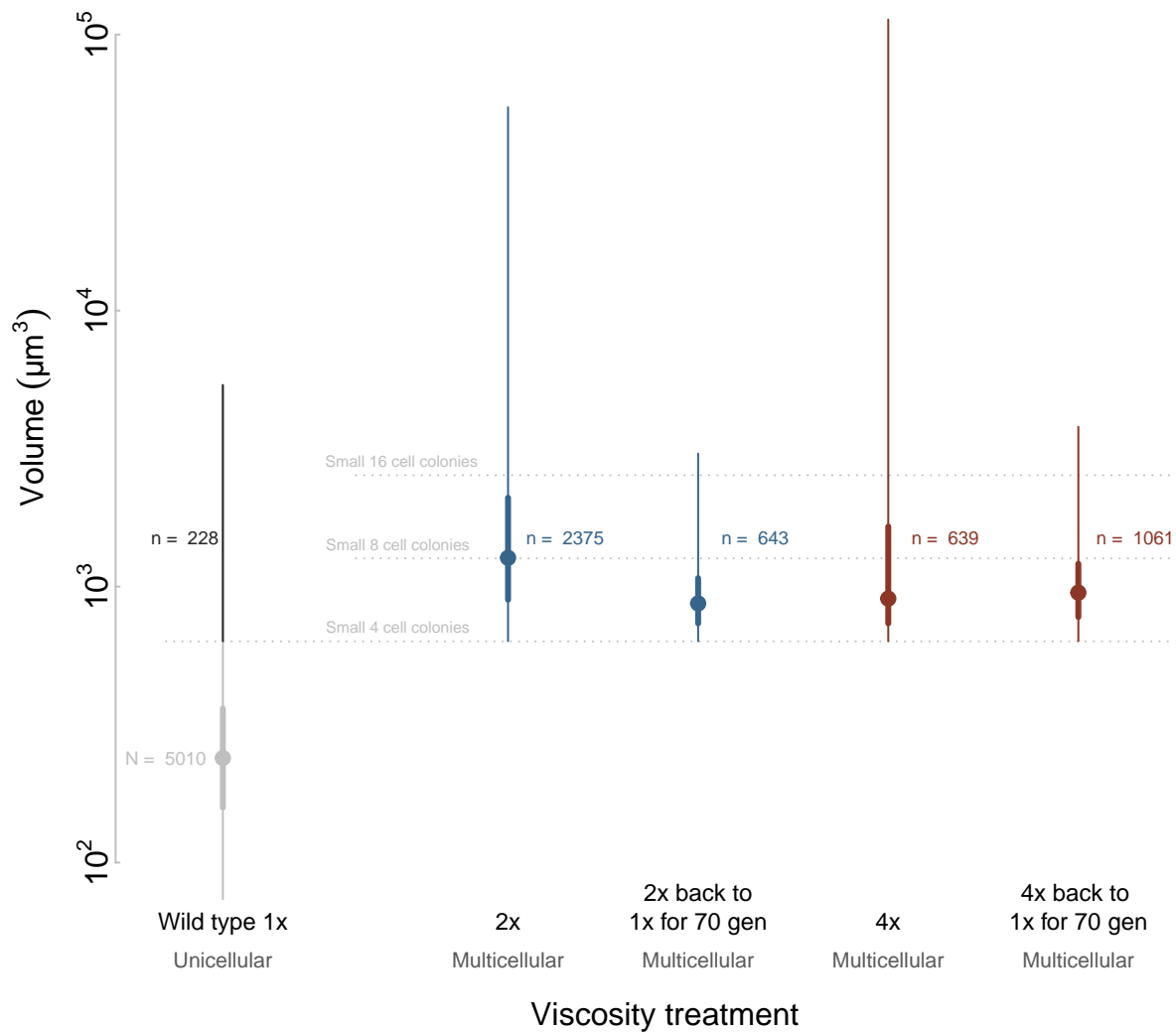


Fig. 5

